JOURNAL OF VIROLOGY, Oct. 1995, p. 6400–6407 Vol. 69, No. 10
0022-538X/95/$04.00+0

An Internal Ribosomal Entry Signal in the Rat VL30 Region of the Harvey Murine Sarcoma Virus Leader and Its Use in Dicistronic Retroviral Vectors

CLARISSE BERLIOZ, CHRISTOPHE TORRENT, AND JEAN-LUC DARLIX*

LaboRétro, Unité de Virologie Humaine-U412, Institut National de la Santé et de la Recherche Médicale, Ecole Normale Supérieure de Lyon, 69364 Lyon Cedex 07, France

Received 27 March 1995/Accepted 18 July 1995

The genetic organization of the 5′ genomic RNA domain of the highly oncogenic Harvey murine sarcoma virus appears to be unusual in that a multifunctional untranslated leader precedes the v-*ras* oncogene. This 5′ leader is 1,076 nucleotides in length and is formed of independent regions involved in key steps of the viral life cycle: (i) the Moloney murine leukemia virus 5′ repeat, untranslated 5′ region, and primer binding site sequences necessary for the first steps of proviral DNA synthesis, (ii) the virus-like 30S (VL30)-derived sequence containing a functional dimerization-packaging signal (E/DLS) directing viral RNA dimerization and packaging into MLV virions, and (iii) an *Alu*-like sequence preceding the 5′ untranslated sequence of v-*ras*^{H} which contains the initiation codon of the p21^{ras} oncoprotein. These functional features, the unusual length of this leader (1,076 nucleotides), and the presence of stable secondary structures between the cap and the v-*ras* initiation codon might well cause a premature stop of the scanning ribosomes and thus inhibit v-*ras* translation. In order to understand how Harvey murine sarcoma virus achieves a high level of expression of the *ras* oncogene, we asked whether the rat VL30 sequence, 5′ to v-*ras*, could contribute to an efficient synthesis of the *ras* oncoprotein. The implications of the VL30 sequence in the translation initiation of Ha-*ras* were investigated in the rabbit reticulocyte lysate system and in murine cells. Results show that the rat VL30 sequence allows a cap-independent translation of a downstream reporter gene both in vitro and in murine cells. Additional experiments performed with dicistronic *neo* · VL30 · *lacZ* mRNAs indicate that the 5′ VL30 sequence (positions 380 to 794) contains an internal ribosomal entry signal. This finding led us to construct a new dicistronic retroviral vector with which the rat VL30 sequence was able to direct the efficient expression of a 3′ cistron and packaging of recombinant dicistronic RNA into murine leukemia virus virions.

The Harvey murine sarcoma virus (HaMSV) is a rat-derived acute transforming retrovirus that carries a *ras* oncogene (v-*ras*^{H}) and induces focal transformation of NIH 3T3 cells and fibrosarcomas and splenic erythroleukemia in animals (58). This virus arose on passaging of Moloney murine leukemia virus (MoMLV) in rats (19), and most probably resulted from multiple recombinations between MoMLV sequences, rat retrotransposon virus-like 30S (VL30) sequences, and the cellular c-*ras* gene (3, 62). In HaMSV, the 1-kb v-*ras*^{H} oncogene is flanked by 3.5 kb of rat-derived virus-like 30S (VL30) sequences (see Fig. 1A) (61).

VL30 elements are present at about 100 copies per haploid genome in rats and mice (3) and share features with endogenous retroviruses, including regions of sequence similarity to the retroviral *gag*, *pol*, and long terminal repeat regions (36, 48). However, no VL30 gene products have yet been identified, and the coding potential of these elements is unknown.

The genetic organization of the 5′ sequences of the HaMSV genomic RNA appears to be original in that a multifunctional 5′ leader precedes the v-*ras* oncogene. The leader is formed of independent domains involved in key steps of the viral life cycle: (i) the MoMLV-derived sequences (positions +1 to 206) which form the 5′ structured domain required for the first steps of proviral DNA synthesis with the repeat, 5′ untranslated region, and primer binding site sequences (11, 41); (ii) the VL30-derived sequence (positions 207 to 927) with a dimerization-packaging signal, called VL30 E/DLS, required for viral RNA dimerization in vitro and packaging into murine leukemia virus (MLV) virions (54, 55); (iii) an *Alu*-like sequence preceding the 5′ untranslated region of v-*ras*^{H} (positions 907 to 1076) which contains the initiation codon (position 1076) of the HaMSV p21^{ras} oncoprotein (58).

Translation initiation of most eukaryotic mRNAs is cap dependent and appears to proceed through a scanning mechanism during which the 40S ribosomal subunit associated with Met-tRNA and initiation factors recognizes the 5′ cap and subsequently migrates along the mRNA until encountering an AUG codon in a favorable context, i.e. (A/G)CCAUGG (28, 31). Translation efficiency can be influenced by sequences between the cap and the translation start site (27, 30). However, this scanning model may not explain translation of RNAs with a 5′ leader containing regions of stable secondary structures (27, 30).

HaMSV genomic RNA contains a very long leader (1,076 nucleotides [nt]) formed of regions with stable secondary structures (15, 41). The MoMLV-derived 5′ first 206 nt have a potential RNA secondary structure with a stability in the range of −50 kcal/mol (ca. −210 kJ/mol) (7, 14a). In addition, two other structured domains are found in the leader: the VL30 transactivation response-like element located between positions 234 and 310 of HaMSV, which has similarity to the transactivation response element of human immunodeficiency virus type 1 (15), and the E/DLS-structured domain of VL30 (positions 205 to 380) (53a). Consequently, the long HaMSV 5′ leader with stable secondary structures between the cap site

* Corresponding author. Mailing address: LaboRétro, Unité de Virologie Humaine INSERM-ENS U412, Ecole Normale Supérieure de Lyon, 46 Allée d'Italie, 69364 Lyon Cedex 07, France. Phone: (33) 72 72 81 69. Fax: (33) 72 72 86 86.

and the v-*ras* initiation codon may well inhibit the initiation of v-*ras* translation by halting or stopping the scanning of 40S ribosomes.

In an attempt to understand the mechanism by which the Ha-ras oncoprotein is expressed at a high level (58), we postulated that the VL30 sequence located in the 5′ leader of HaMSV might promote an efficient translation of the Ha-*ras* oncogene. The possible implication of this VL30 sequence in the translation initiation mechanism of Ha-*ras* was investigated in the rabbit reticulocyte lysate system (RRL) and in murine cells. The results indicate that the 5′ VL30 sequence allows a cap-independent translation of a reporter gene and can promote the efficient translation of the second cistron when located between two cistrons in a dicistronic mRNA. Therefore, the 5′ VL30 sequence appears to contain an internal ribosome entry signal.

MATERIALS AND METHODS

Plasmid construction. Standard procedures were used for restriction nuclease digestion and plasmid DNA construction (49). *Escherichia coli* HB101 strain 1035 (*recA* mutant) was used for plasmid DNA amplification. Details of the constructions are given below. All numbering was done with respect to the genomic RNA cap site (position +1).

(i) pVL-D1-380. The VL30 DNA fragment from positions 1 to 380 was generated by PCR (pVL-CG20 template) (55). The PCR fragment was digested with *Nhe*I and inserted between *neo* and *lacZ* of pMLV-CB28 digested by *Nhe*I (7). The *neo* · VL30 · *lacZ* sequences are under the control of the T7 RNA polymerase promoter for in vitro expression and the cytomegalovirus early promoter for expression in eukaryotic cells. In this construct, the initiation of β-galactosidase (β-Gal) translation was under the control of an AUG in a favorable context, i.e., A/GCCAUGG (28), which was created by PCR at position 380 (see Fig. 4).

(ii) pVL-D1-794. The VL30 DNA fragment from positions 1 to 794 was generated by PCR. The PCR fragment was digested by *Nhe*I and inserted between *neo* and *lacZ* of pMLV-CB28 digested by *Nhe*I. In this construct and in pVL-D205-794 and pVL-D380-794, the initiation of β-Gal translation was under the control of an AUG in a favorable context, i.e., A/GCCAUGG (28), which was created by PCR at position 794 (see Fig. 4).

(iii) pVL-D205-794. The VL30 DNA fragment from positions 205 to 794 was generated by PCR. The PCR fragment was digested by *Nhe*I and inserted between *neo* and *lacZ* of pMLV-CB28 digested by *Nhe*I (see Fig. 4).

(iv) pVL-D380-794. The VL30 DNA fragment from positions 380 to 794 was generated by PCR. The PCR fragment was digested by *Nhe*I and inserted between *neo* and *lacZ* of pMLV-CB28 digested by *Nhe*I (see Fig. 4).

(v) pEMCV-D260-837. The encephalomyocarditis virus (EMCV) internal ribosome entry site (IRES) fragment from positions 260 to 837 was generated by PCR and digested by *Nhe*I. This fragment was inserted between the *neo* and the *lacZ* of pMLV-CB28 digested with *Nhe*I. In this construct, the initiation of β-Gal translation was under the control of the 11th AUG of the EMCV leader at position 837 (see Fig. 4).

(vi) pVL-M28-380. The pVL-M1-380 plasmid, which retained the VL30 sequence from positions 28 to 380 and the *lacZ* gene, was generated by digestion with *Hin*dIII and *Sma*I of pVL-D1-380 and ligation of the *Sma*I site with the *Hin*dIII Klenow-filled site. This construct contains the VL30 sequence from positions 28 to 380 upstream of the *lacZ* gene under the control of the cytomegalovirus early promoter and T7 RNA polymerase promoter (see Fig. 1B).

(vii) pVL-M28-794. The pVL-M1-794 plasmid, which retained the VL30 sequence from positions 28 to 794 and the *lacZ* gene, was generated by digestion with *Hin*dIII and *Sma*I of pVL-D1-794 and ligation of the *Sma*I site with the *Hin*dIII Klenow-filled site. This construct contains the VL30 sequence from positions 28 to 794 upstream of the *lacZ* gene under the control of the cytomegalovirus early promoter and T7 RNA polymerase promoter (see Fig. 1B).

(viii) pEMCV-M260-837. To generate the pEMCV-M260-837 plasmid, which retained the EMCV sequence from positions 260 to 837 and the *lacZ* gene, pEMCV-D260-837 was partially digested with *Eco*RI and religated. This construct contains the EMCV sequence (positions 260 to 837) upstream of the *lacZ* gene under the control of the cytomegalovirus early promoter and T7 RNA polymerase promoter (see Fig. 1B).

(ix) pVL-CBT1. The VL30 DNA fragment from positions 205 to 380 was generated by PCR. The PCR fragment was digested with *Nhe*I and inserted between the phosphatase and *neo* genes of pMLV-CB71 (7) digested with *Spe*I. In this construct, the initiation of *neo* translation was under the control of an AUG in a favorable context, i.e., A/GCCAUGG (28), which was created by PCR at position 380 (see Fig. 8A).

(x) pVL-CBT2. The VL30 DNA fragment from positions 205 to 794 was generated by PCR and digested with *Nhe*I. This fragment was inserted between the phosphatase and *neo* genes of pMLV-CB71 digested with *Spe*I. In this construct, the initiation of *neo* translation was under the control of an AUG in a favorable context, i.e., A/GCCAUGG (28), which was created by PCR at position 794 (see Fig. 8A).

(xi) pEMCV-CBT4. The pAPE DNA fragment *Eco*RI-*Eco*RI (gift of F. Flamand) containing the phosphatase gene was cloned into the pLAEN retroviral vector digested with *Eco*RI (positions 1644 and 2866) which contains the EMCV IRES and the *neo* gene (2). In pEMCV-CBT4, the EMCV IRES was flanked by the phosphatase and neomycin genes, and the initiation of *neo* translation was under the control of the 11th AUG of EMCV IRES (position 837; see Fig. 8A).

(xii) pMLP-P2A and pMLP-RP2A. Plasmids pMLP-P2A and pMLP-RP2A contain the poliovirus protease 2A coding sequence derived from poliovirus type 1 (Mahoney strain). In pMLP-P2A, the protease coding sequence was inserted downstream of the adenovirus major late promoter and its tripartite leader. The pMLP-P2AR plasmid containing the insert in the reverse orientation served as a control. These plasmids were gifts of N. Fouillot (16).

(xiii) pβ-actin-LacZ. The pβ-actin-LacZ plasmid contains the *lacZ* gene under the control of the β-actin promoter. This plasmid was a gift of P. Savatier (50).

In vitro-generated RNA. Five micrograms of plasmid DNA linearized with *Xba*I was transcribed in 0.1 ml of 40 mM Tris-HCl (pH 7.5)–6 mM $MgCl_2$–2 mM spermidine–10 mM dithiothreitol–10 mM NaCl–0.5 mM each ribonucleoside triphosphate with 40 U of T7 RNA polymerase and 80 U of the RNase inhibitor RNasin for 3 h at 37°C. Following DNase treatment (RQ1 DNase), the RNA was extracted with phenol-chloroform and precipitated with ethanol. After being washed with 70% ethanol, the RNA was dissolved in sterile bidistilled water. To synthesize capped RNAs, the reactions were carried out under the same conditions described above, except that ATP, CTP, and UTP were added at a final concentration of 0.5 mM with 0.05 mM GTP and 0.5 mM $m^7G(5')ppp(5')Gm$ (Pharmacia). RNA generated in vitro was analyzed by electrophoresis through a 0.7% (wt/vol) agarose gel in 50 mM Tris–borate (pH 8.3)–0.1 mM EDTA at 5 V/cm and visualized by ethidium bromide staining (1 μg/ml for 5 min).

In vitro translation. Capped and uncapped monocistronic RNAs were translated in the nuclease-treated RRL (Promega) at 50% of the original concentration with 10 μg of RNA per ml and 1 mCi of [^{35}S]methionine per ml (Amersham) at 31°C for 1 h. These assays were supplemented with potassium acetate to a final concentration of 130 mM.

Monocistronic RNAs were also translated in the Flexi RRL (Promega) at 66% of the original concentration under the same conditions described above. These assays were supplemented with either potassium acetate or potassium chloride to a final concentration of 40, 80, or 120 mM.

Dicistronic RNAs were translated with the RRL assay as described above. These assays were supplemented with potassium acetate (KAc) to a final concentration of 60 mM and with potassium chloride to a final concentration of 40 mM.

The reaction mixtures were then boiled in 62.5 mM Tris-HCl (pH 6.8)–2% sodium dodecyl sulfate (SDS)–10% glycerol–5% β-mercaptoethanol–0.02% bromophenol blue, and the ^{35}S-labelled proteins were analyzed by 0.2% SDS–10% (wt/vol) polyacrylamide gel electrophoresis. The efficiencies of neomycin and β-Gal translation were quantitated by means of scanning with Cirrus 1.0.1 (Softhansa GmbH) and scan analysis (version 2.0; Biosoft). The efficiencies of IRES-mediated translation initiation were determined by the ratio of β-Gal expression to neomycin expression.

Cell culture and DNA transfection. NIH 3T3 cells were grown in Dulbecco modified Eagle medium containing 5% newborn calf serum at 37°C in the presence of 5% CO_2. NIH 3T3 cells were seeded at 5×10^5 cells per 100-mm-diameter plate 24 h prior to transfection. The cells were transfected by the calcium phosphate procedure exactly as described previously (10). Transfections were performed in duplicate for each plasmid with 6 μg of the pVL DNA construct. Two days later, the transfected cells were washed. At 24 h after transfection, transfected cells were pooled to determine the β-Gal activity and lysed to extract the RNAs for Northern analysis. The efficiency of IRES-mediated translation initiation was determined by the ratio of β-Gal activity to the level of scanned mRNA *lacZ* (in arbitrary units). Cotransfection experiments with protease 2A were performed in duplicate for each plasmid combination with 5 μg of plasmid pMLP-P2A or pMLP-P2AR and either 7 μg of pVL or 10 μg of pβ-actin-LacZ by plating. Three days later, proteins from the transfected cells were extracted for the assay of β-Gal activity, and cellular RNAs were subjected to Northern analysis. The efficiency of β-Gal expression was determined by the ratio of β-Gal activity to the level of arbitrary units of scanned mRNA *lacZ*.

β-Gal enzyme assays were performed on cell extracts by using the β-Gal enzyme assay system (Promega).

Transfections and infections with dicistronic retroviral vectors. GP+E-86 cells (37) were seeded at 5×10^5 cells per 100-mm-diameter plate 24 h prior to transfection. The cells were transfected by the calcium phosphate procedure (10) with 20 μg of pVL-CBT1, pVL-CBT2, or pEMCV-CBT4. After 3 days, the virus-containing media were harvested and cells were fixed for alkaline phosphatase histochemical staining or placed under G418 selection at 0.8 mg/ml for 4 weeks.

All retroviral infections or titrations were performed by adding diluted virus-containing medium to the cells. One day prior to infection, NIH 3T3 cells were seeded at 1.5×10^5 cells per 30-mm-diameter plate. Freshly harvested viruses from transient expression of helper cells were filtered (0.45-μm-pore-size filter), and Polybrene was added at a concentration of 8 μg/ml. Infected cells were grown for 24 h. Before their passage, infected cells were either placed under

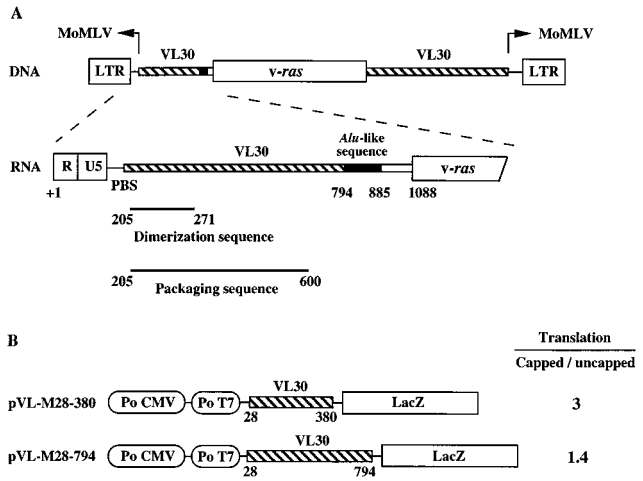

FIG. 1. Map of 5′ end of HaMSV RNA and influence of 5′ cap on VL30 · *lacZ* mRNA translation in RRL. (A) Schematic representation of 5′ end of HaMSV RNA. Numbering is done with respect to the genomic RNA cap site (position +1). R, U5, and PBS are the repeat, the untranslated 5′ region, and the primer $tRNA^{Pro}$ binding site used to initiate the synthesis of minus-strand DNA, respectively. The boundaries of the MoMLV, VL30, *Alu*-like, and *ras* sequences are shown above the proviral DNA. The VL30 dimerization and packaging sequences are indicated. LTR, long terminal repeat. (B) Cap influence on VL30 · *lacZ* mRNA translation in RRL. Monocistronic pVL-M28-380 and pVL-M28-794 plasmids contain the rat VL30 sequence of HaMSV upstream of the *lacZ* gene and under the control of the T7 RNA polymerase promoter (Po T7) and the cytomegalovirus early promoter (Po CMV). Capped and uncapped pVL-M28-380 and pVL-M28-794 mRNAs were translated in the RRL at a concentration of 10 μg/ml in the presence of [^{35}S]methionine (see Materials and Methods). The effect of the cap on global translation of each VL30 · *lacZ* mRNA is indicated on the right. Capped/uncapped is the ratio of translation efficiencies of capped versus uncapped RNAs.

G418 selection at 0.8 mg/ml for 2 weeks or stained for detection of expression of alkaline phosphatase (see below).

Preparation of cellular RNAs and Northern analysis. Extraction of cellular RNAs from transfected cells and Northern analysis were performed on transfected and infected cells as described previously by Khandjian and Meric (26). A ^{32}P-labelled probe complementary to the *lacZ* gene (positions 23 to 436) (25) was labelled by using the NonaPrimer Kit I (Appligene). The membrane was autoradiographed overnight at −80°C. RNAs were quantitated by means of scanning with Cirrus 1.0.1 (Softhansa GmbH) and scan analysis (version 2.0; Biosoft). The level of *lacZ* mRNA expressed was given in arbitrary units by fixed area scanning on the same autoradiography.

Alkaline phosphatase histochemical staining. After transfection or infection, cells were fixed with 2% formaldehyde and 0.2% glutaraldehyde, washed two times with phosphate-buffered saline (PBS), and incubated for 30 min in PBS at 65°C. Then, the cells were washed two times with phosphatase buffer containing 100 mM Tris-HCl (pH 9.5)–100 mM NaCl–50 mM $MgCl_2$ and incubated for 3 h in a staining solution containing 0.1 mg of 5-bromo-4-chloro-3-indolylphosphate (BCIP) per ml, 1 mg of nitroblue tetrazolium salt per ml, and 1 mM levamisole in phosphate buffer.

RESULTS

Effect of 5′ cap VL30 · *lacZ* RNA expression in RRL. To examine the possibility that the VL30 sequence present in the HaMSV 5′ leader might influence translation initiation, VL30 · *lacZ* RNAs were synthesized in vitro and further translated in the nuclease-treated RRL. In vitro-generated capped and uncapped 5′ VL30 · *lacZ* RNAs containing the VL30 sequence from positions 28 to 380 (pVL-M28-380) or most of the 5′ VL30 sequence (positions 28 to 794; pVL-M28-794) were translated in the nuclease-treated RRL supplemented with potassium acetate at a final concentration of 130 mM (58) (Fig. 1B). The results indicate that capped VL30(28-380) · *lacZ* RNA was translated about three times more efficiently than uncapped RNA (Fig. 1B). Interestingly, uncapped VL30(28-794) · *lacZ* RNA with most of the VL30 sequence found in the HaMSV 5′ leader was translated at a level similar to that of capped RNA (Fig. 1B). These findings show that translation of VL30(28-794) · *lacZ* RNA is largely cap independent.

Influence of potassium salts on VL30 · *lacZ* RNA expression in RRL. In vitro translation of mRNA appears to be more efficient in the presence of KAc rather than potassium chloride (KCl) (60), most probably resulting from the binding inhibition of the small ribosomal subunit to the mRNA caused by Cl^- ions at or above 50 mM (60). In contrast, Jackson reported that translation of EMCV RNA exhibited a salt optimum level that was unusually high for an uncapped mRNA and that it was more accurate with KCl than KAc (22). In addition, these investigators reported that EMCV RNA translation responded to various salts in a way that was possibly related to the translation initiation of EMCV RNA via an internal ribosome entry mechanism.

These observations prompted us to investigate the influence of KCl and KAc on the in vitro translation of monocistronic VL30 · *lacZ* RNAs. In vitro-generated RNAs VL30(28-380) · *lacZ* and VL30(28-794) · *lacZ* (Fig. 1B) were translated in the Flexi RRL (Promega). In addition, we used the EMCV(260-837) · *lacZ* RNA as a positive control for translation in the presence of high concentrations of KCl. These assays were supplemented with either KAc or KCl to a final concentration of 40, 80, or 120 mM. Expression of β-Gal was optimal for both VL30 and EMCV *lacZ* RNAs at 40 mM KAc (data not shown). As expected, with KCl, synthesis of β-Gal was optimal for EMCV(260-837) · *lacZ* RNA at 120 mM KCl (Fig. 2, lane 11). With VL30(28-380) · *lacZ* RNA, a concentration of 40 mM promoted a high level of β-Gal synthesis (Fig. 2, lane 3). However, in the presence of a higher level of KCl (80 or 120 mM), β-Gal expression was completely inhibited (Fig. 2, lanes 4 and 5). Interestingly, translation of VL30(28-794) · *lacZ* RNA gave rise to high levels of β-Gal synthesis at both 80 and 120 mM KCl (Fig. 2, lanes 7 and 8). Moreover, incomplete β-Gal products were much less abundant at KCl concentrations at or above 80 mM with this RNA (Fig. 2, compare lanes 6, 7, and 8). These results indicate that the VL30(28-794) · *lacZ* RNA, like EMCV(260-837) · *lacZ* RNA, can be efficiently translated in the presence of a high concentration of Cl^- ions thought to inhibit translation initiation (22).

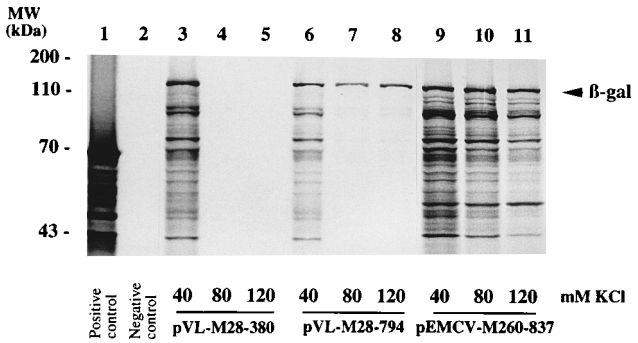

FIG. 2. Influence of potassium salts on in vitro expression of monocistronic 5′ VL30 · *lacZ* RNAs. Monocistronic VL30(28-380) · *lacZ* (lanes 3 to 5), VL30(28-794) *lacZ* (lanes 6 to 8) and EMCV(260-837) · *lacZ* (lanes 9 to 11) RNAs were translated in the Flexi RRL (Promega) at 66% of the original concentration at a concentration of 10 μg/ml in the presence of [^{35}S]methionine (see Materials and Methods). These assays were supplemented with potassium chloride to a final concentration of 40 mM (lanes 3, 6, and 9), 80 mM (lanes 4, 7, and 10) or 120 mM (lanes 5, 8, and 11). After heat denaturation, ^{35}S-labelled proteins were analyzed by 0.2% SDS–7% (wt/vol) polyacrylamide gel electrophoresis. The position of β-Gal (110 kDa) is indicated. Lanes: 1, luciferase RNA; 2, no RNA.

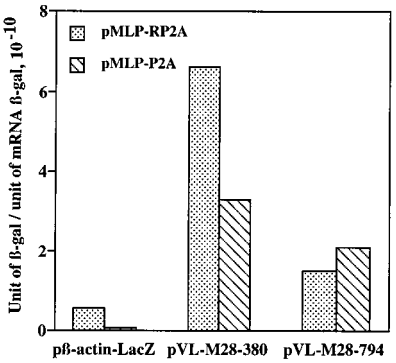

FIG. 3. Effect of poliovirus protease 2A on translation of monocistronic VL30 · *lacZ* mRNA. Plasmids pVL-M28-380 and pVL-M28-794 contain the rat VL30 sequence upstream of the *lacZ* gene. In pβ-actin-LacZ, β-Gal expression is driven by the rat β-actin promoter. Plasmid pMLP-P2A codes for the poliovirus protease 2A under the control of the adenovirus major late promoter (MLP); pMLP-RP2A has the p2A sequence in the reverse orientation as a control. Cotransfection experiments with protease 2A were performed in duplicate for each plasmid combination. After 48 h, β-Gal activity was assayed on transfected cells, and cellular RNAs were extracted for Northern analysis. Efficiencies of translation are given as units of β-Gal per arbitrary unit of mRNA β-Gal. The results given are the averages for three independent experiments.

Influence of poliovirus protease 2A on expression of VL30 · *lacZ* RNAs. In poliovirus, ribosomes can directly bind to sequences within the 5′ untranslated region of the uncapped viral RNA and then scan to the initiation codon while translation of cellular mRNAs is inhibited by inactivation of the cap-binding complex eIF-4F, a process mediated by poliovirus protease 2A (20). In previous studies, transient expression of protease 2A was found to cause an inhibition of cap-dependent translation (7, 16).

To examine whether VL30 sequences contain an element conferring cap-independent translation initiation in murine cells, DNA vectors expressing VL30 · *lacZ* RNA (Fig. 1B) were cotransfected into NIH 3T3 cells with a plasmid expressing the poliovirus protease 2A. In the latter plasmid, the poliovirus protease 2A-coding region was inserted downstream of the adenovirus major late promoter, and its tripartite leader permitted the translation of this mRNA independently of the formation of the cap-binding complex (13, 16). The pMLP-P2A vector contains the insert in the correct orientation allowing the expression of protease 2A while pMLP-RP2A contains the insert in the reverse orientation serving as the control. In pVL-M28-380 and pVL-M28-794, the VL30 sequences were inserted upstream of the *lacZ* reporter gene (see Materials and Methods) (Fig. 1B). In addition, we used the β-actin-*lacZ* plasmid as a positive control for a cap-dependent translation process. Two days after cotransfection into murine cells, β-Gal activity was assayed in transfected cells, and cellular RNAs were extracted for Northern analysis. The efficiencies of translation were determined as units of β-Gal activity per arbitrary unit of *lacZ* mRNA (Fig. 3).

The level of β-Gal activity in cells cotransfected with pβ-actin-LacZ and pMLP-P2A was eight times lower than the level in cells cotransfected with pMLP-P2AR (Fig. 3). These results indicate that poliovirus protease 2A encoded by the pMLP-P2A vector was capable of strongly inhibiting the cap-dependent synthesis of β-Gal. Coexpression of VL30(28-380) · *lacZ* and MLP-P2A RNAs in murine cells resulted in a 2.5-fold decrease of β-Gal synthesis compared with that in the absence of protease 2A (pMLP-RP2A) (Fig. 3). Interestingly, coexpression of VL30(28-794) · *lacZ* and MLP-P2A RNAs did not decrease but slightly increased β-Gal synthesis compared with that in the absence of protease 2A (Fig. 3). This finding clearly suggests that translation initiation of VL30(28-380) · *lacZ* RNA is mostly cap independent.

In vitro expression of dicistronic *neo* · 5′ VL30 · *lacZ* mRNAs. Cap-independent initiation of translation is well documented for a variety of viral (4, 7, 52, 53, 57) and cellular RNAs (34, 44, 57a) and appears to proceed via an internal ribosome entry mechanism (23). IRESs are found in the naturally uncapped RNAs of picornaviruses (9, 18, 23, 24, 45, 47) and are formed of highly structured RNA elements which, in conjunction with cellular proteins, direct ribosomes to the AUG initiation codon or to an internal position upstream of the start codon (23).

In HaMSV genomic RNA, the 5′ leader is very long (1,076 nt) and is formed of regions with stable secondary structures (see introduction) (Fig. 1). The ability of the 5′ leader sequence from positions 28 to 794 to promote cap-independent translation suggests that initiation of the Ras oncoprotein might occur by direct binding of ribosomes to the 5′ VL30 sequence. To investigate this possibility, the 5′ VL30 sequence (positions 1 to 794) was inserted between the neomycin (*neo*) and the β-Gal (*lacZ*) reporter genes (Fig. 4) (see Materials and Methods). The recombinant pVL plasmids allowed in vitro synthesis of dicistronic RNAs ranging from 4,600 to 5,000 nt in length (Fig. 4). Agarose gel electrophoresis of the in vitro-generated RNAs confirmed that they were intact and unique (data not shown).

Subsequently, the dicistronic RNAs were translated in the RRL system. These RNAs encoded Neo protein directing standardization of the level of translation and β-Gal with an average molecular mass of 110 kDa. This system allows β-Gal expression only when an IRES is present in the 5′ VL30 RNA sequence (Fig. 5). The positive control employed RNA coding for luciferase (65 kDa; lane 1), and the negative control corresponded to translation without RNA (lane 2). The EMCV IRES served as a positive IRES control (24). Indeed, the EMCV IRES directed efficient β-Gal expression of the second cistron (lane 4, position of β-Gal) though at a lower level (0.6 fold lower) than the first cistron (lane 4, position of *neo*). Translation of the dicistronic *neo* · 5′ VL30 · *lacZ* RNA with the VL30 sequence (positions 1 to 794) inserted between the *neo* and *lacZ* genes produced β-Gal (lane 6) at a level similar to that of 5′ VL30 · *lacZ* RNA (lane 3). In this experiment, the β-Gal/*neo* ratio was similar to that observed with the *neo* · EMCV IRES · *lacZ* RNA (0.6-fold). These data strongly suggest that ribosomes can recognize the 5′ VL30 sequence and directly initiate β-Gal synthesis. When the 5′ first 205 nt of the HaMSV leader were deleted (pVL-D205-794 construct),

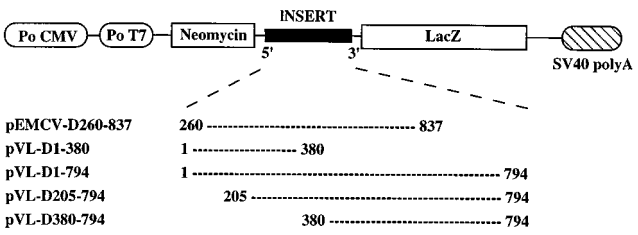

FIG. 4. Dicistronic plasmid DNA constructs for in vitro and in vivo expression. Dicistronic plasmid DNAs contain the rat VL30 sequence of the HaMSV leader or the EMCV leader between the neomycin and β-Gal genes under the control of the T7 RNA polymerase promoter (Po T7) for in vitro experiments and the cytomegalovirus early promoter (Po CMV) for in vivo expression. The viral DNA fragments cloned in the plasmids are shown (numbering is done with respect to the +1 cap site of the viral RNA). SV40, simian virus 40.

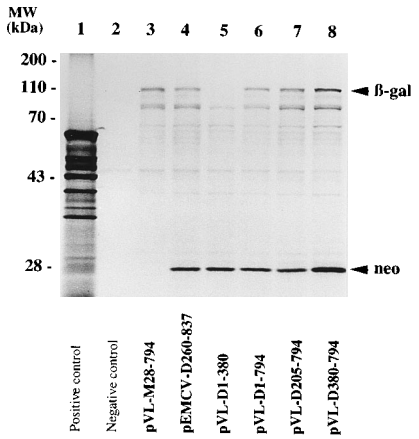

FIG. 5. Translation of monocistronic and dicistronic 5′ VL30 RNAs in RRL. Lanes: 1 and 2, positive (luciferase plasmid DNA; Promega) and negative (no plasmid DNA) controls, respectively; 3 to 8, pVL-M28-794, pEMCV-D260-837, pVL-D1-380, pVL-D1-794, pVL-D205-794, and pVL-D380-794 RNAs, respectively, expressed in the RRL (Promega). After heat denaturation, ^{35}S-labelled proteins were analyzed by 0.2% SDS–12% (wt/vol) polyacrylamide gel electrophoresis. The positions of the *neo* (28-kDa) and β-Gal (110-kDa) proteins are indicated. Lower-molecular-mass bands (indicated on the left) correspond to premature translation stops.

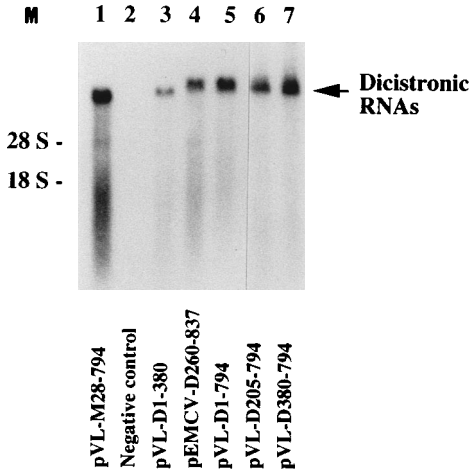

FIG. 6. Synthesis of VL30-derived dicistronic mRNAs in NIH 3T3 cells. Total RNA was extracted from NIH 3T3 cells transfected with 6 μg of plasmid pVL-M28-794, pVL-D1-380, pEMCV-D260-837, pVL-D1-794, pVL-D205-794, or pVL-D380-794 DNA. VL30 RNAs were subjected to electrophoresis in a 0.7% agarose–formaldehyde gel in morpholinopropanesulfonic acid buffer and transferred to nitrocellulose. Hybridization was conducted with a ^{32}P-labelled probe corresponding to positions 23 to 436 of *lacZ*. The 18S and 28S rRNAs were revealed by ethidium bromide staining prior to RNA transfer and hybridization. The positions of the 18S and 28S rRNAs and of the dicistronic *neo* · MLV · *lacZ* RNAs are indicated.

the level of β-Gal synthesis was similar to that observed with the first construct (pVL-D1-794) (ratio, 0.7-fold; lane 7), indicating that sequence between positions 1 and 205 had little influence on the mechanism of internal translation initiation. On the other hand, the construct containing only the sequence between positions 1 and 380 produced a very low level of β-Gal (pVL-D1-380 construct) (lane 5), indicating that this region alone is unable to promote internal translation initiation. Interestingly, insertion of the VL30 sequence from positions 380 to 794 (pVL-D380-794 construct) (lane 8) allowed a high level of β-Gal synthesis, corresponding to a β-Gal/*neo* ratio of 0.7 fold, similar to that obtained with the complete 5′ VL30 sequence and the EMCV IRES. These results strongly suggest that the VL30 sequence between positions 380 and 794 can promote initiation of translation via an internal ribosome entry mechanism.

Expression of dicistronic *neo* · 5′ VL30 · *lacZ* DNA constructs in NIH 3T3 cells. In order to confirm the in vitro data, expression of the dicistronic pVL DNA plasmids was examined in cell culture by means of DNA transfection and the subsequent quantitation of β-Gal activity and Northern analysis of dicistronic RNAs.

To rule out the possibility that a cryptic promoter and/or cryptic splice sites could function with the dicistronic pVL plasmids used, cellular RNAs were extracted 2 days after transfection and subjected to Northern analysis using a ^{32}P-labelled *lacZ* probe (see Materials and Methods). As shown in Fig. 6, only one major RNA was detected at the expected size by Northern analysis in NIH 3T3 cells transfected with the dicistronic pVL DNA constructs. If a cryptic promoter and/or cryptic splice site had been used, an mRNA of at least 3,000 nt (*lacZ* gene is 3,078 bp) (25) should have been detected between the 18S (1,900 nt) and the 28S (4,700 nt) RNAs. Since no RNA was observed in this region or outside of the region presented, the *neo* · VL30 · *lacZ* RNAs were dicistronic under our in vivo assay conditions.

NIH 3T3 cells were transfected with dicistronic pEMCV and pVL plasmids, and the efficiency of translation of the second cistron was determined as units of β-Gal per arbitrary unit of dicistronic β-Gal mRNA (see Materials and Methods) (Fig. 7). The pEMCV-D260-837 positive control, where the EMCV IRES directed the synthesis of β-Gal in dicistronic *neo* · EMCV · *lacZ* mRNA, allowed the synthesis of 5.5×10^{-10} U of β-Gal per arbitrary unit of mRNA β-Gal (Fig. 7). With the dicistronic vector containing the 5′ VL30 sequence (pVL-D1-794) between the two reporter genes, the level of

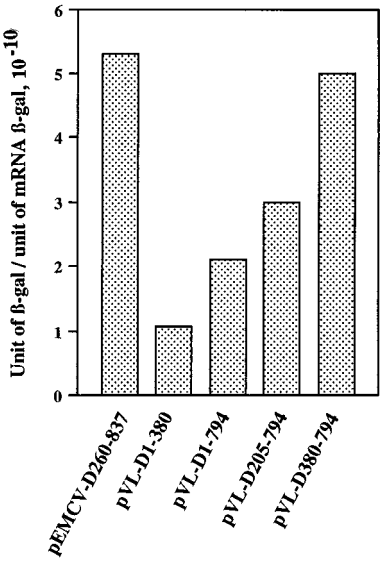

FIG. 7. Expression of rat *neo* · VL30 · *lacZ* RNAs in murine cells. NIH 3T3 cells (5×10^5 cells per 100-mm-diameter plate) were transfected with pEMCV-D260-837, pVL-D1-380, pVL-D1-794, pVL-D205-794, or pVL-D380-794 in duplicate by means of the calcium phosphate procedure. Two days after transfection, cells of one plate were either pooled for determination of β-Gal activity or lysed for extraction of RNAs for Northern analysis. The efficiency of IRES-mediated protein synthesis is expressed as units of β-Gal per arbitrary unit of mRNA *lacZ*. The results are the averages for three experiments (± 5%).

A

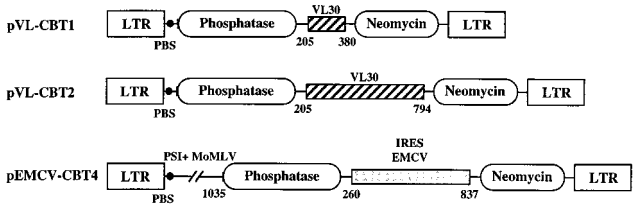

B

Plasmid construct	number of Neo^{r}foci/ 1000 transfected cells	viral titer (10^4cfu/ml)	% of Neo^r/Pa$^+$ infected cells
pVL-CBT1	120	0.02	0
pVL-CBT2	360	1.5	97
pEMCV-CBT4	750	3	98

FIG. 8. Dicistronic MLV-derived retroviral vectors with rat 5′ VL30 sequences promoting internal initiation of translation and packaging. (A) The pVL-CBT dicistronic retroviral vectors were constructed with the rat 5′ VL30 sequence of HaMSV between the phosphatase and neomycin cistrons flanked by the MLV long terminal repeats (LTR). The VL30 DNA fragments used in the constructs are shown. In these vectors, the 5′ sequences contain the repeat, the untranslated 5′ region, the primer binding site (PBS), and SD elements while the dimerization/encapsidation signal (E/DLS) from positions 205 to 794 was located between the two reporter cistrons. The pEMCV-CBT4 dicistronic vector was used as a positive control and contains the EMCV IRES between the phosphatase and neomycin cistrons. The E/DLS or Psi+MLV (5) is located at the 5′ end of this vector and extended to position 1040. (B) Data from two independent experiments. The viral titer of each recombinant virus is reported in CFU per milliliter of collected medium. The efficiency of protein synthesis corresponded to the number of Neo^r foci expressing the phosphatase gene per 1,000 transfected cells. The percentage of infected foci expressing the two genes was calculated as the ratio of infected G418^r foci expressing the indicator gene (phosphatase) after 2 weeks of G418 selection to the number of infected G418^r foci.

β-Gal activity obtained was 2.6 times less than that obtained with the dicistronic vector containing the EMCV IRES (Fig. 7). Deletion of nt 1 to 205 and nt 1 to 380 (pVL-D205-794 and pVL-D380-794, respectively) (Fig. 7) resulted in 1.4- and 2.2-fold increases in β-Gal activity, respectively (Fig. 7, compare pVL-D205-794 to pVL-D1-794 and pVL-D380-794 to pVL-D1-794). It should be noted that β-Gal expression by using the dicistronic construct retaining only the 5′ VL30 sequence from positions 380 to 794 (pVL-D380-794) was almost as efficient as the pEMCV-D260-837 construct. On the other hand, the dicistronic vector containing the HaMSV 5′ leader from positions 1 to 380 (pVL-D1-380) promoted only a low level of β-Gal synthesis. Taken together, these results strongly suggest that the rat VL30 retrotransposon contains an internal ribosome entry signal between positions 380 and 794 and that the sequence from positions 1 to 380 of the HaMSV 5′ leader had a negative effect on this VL30 IRES function in murine cells, as described for the poliovirus (46).

New MLV-VL30-derived vector with VL30 sequences having both translation and encapsidation functions. The finding that 5′ VL30 sequences contain a functional internal ribosome entry signal prompted us to construct a new dicistronic retroviral vector. In this construct, VL30 sequences (positions 205 to 794 or 205 to 380) were inserted between the phosphatase and neomycin genes (Fig. 8A, pVL-CBT2 and pVL-CBT1, respectively) flanked by the MLV 5′ long terminal repeat and primer binding site sequences and by the 3′ long terminal repeat, respectively. As a positive control, we used the pEMCV-CBT4 dicistronic vector where the EMCV IRES (24) was inserted between the phosphatase and neomycin genes. It should be noted that the Psi+ sequence (also called E/DLS) (positions 212 to 1040) is present in pEMCV-CBT4 and is known to promote a 10- to 30-fold increase in MLV-derived RNA packaging compared with that in RNA containing only the MLV 5′ leader (1, 6).

Ecotropic GP-E+86 helper cells were transfected with these MLV VL30-derived retroviral vectors, and short-term expression of phosphatase as well as long term expression of neomycin by the transfected helper cells was monitored (see Materials and Methods). The number of transfected helper cells was measured by means of the short-term expression of phosphatase (data not shown). After 2 weeks of G418 selection (see Materials and Methods), the number of Neo^r foci expressing the phosphatase gene per 1,000 transfected cells was 360 with the MLV VL30 dicistronic vector (pVL-CBT2) and thus two times less than the 750 Neo^r foci obtained with the MLV-Psi$^+$-EMCV vector (pEMCV-CBT4). The number of Neo^r foci was no more than 120 with the dicistronic vector containing the VL30 fragment from positions 205 to 380 (pVL-CBT1; Fig. 8B). These results are in agreement with those obtained with the dicistronic *neo* · VL30 · *lacZ* DNA constructs in NIH 3T3 cells.

The 5′ VL30 sequence of HaMSV contains the packaging Psi (or E/DLS) sequence, which is a *cis*-acting element necessary for the specific encapsidation of the genomic HaMSV RNA and VL30-derived RNA in MLV virions (54, 55). To investigate the ability of the 5′ VL30 sequence inserted between two genes in a retroviral vector to direct RNA packaging, the recombinant viruses transiently expressed by the helper cells were used to infect fresh NIH 3T3 cells. The titer of the dicistronic pVL-CBT2 vector was found to be about 1.5 $\times$ 10^4 CFU/ml (Fig. 8B). This is about two times less than that of the pEMCV-CBT4 vector containing the Psi+ packaging signal and the EMCV IRES element (Fig. 8B). The titer of the dicistronic pVL-CBT1 vector with the HaMSV leader from positions 205 to 380 was 150 times less than that of the pEMCV-CBT4 vector (Fig. 8B).

The infected NIH 3T3 cells were put under G418 selection to monitor long-term expression of neomycin and phosphatase. As shown in Fig. 8B, 97 or 98% of the pVL-CBT2 or pEMCV-CBT4 infected Neo^r foci, respectively, expressed phosphatase. It should be noted that the expression of the two genes was stable after 30 days of G418 selection. In conclusion, these results show that the 5′ VL30 sequence (positions 205 to 794) inserted between two genes provides an IRES for efficient translation and an E/DLS signal for packaging of RNA into MLV virions.

DISCUSSION

One important feature of retroviruses such as HaMSV, MLV, spleen necrosis virus, Rous sarcoma virus, and human immunodeficiency virus type 1 is the presence of a long leader at the 5′ end of the genomic RNA (350 to 1,076 nt), with stable secondary structures involved in key steps of the viral life cycle, such as the initiation of reverse transcription, the dimerization and encapsidation of the unspliced genomic RNA, and the initiation of protein synthesis (5, 11, 12, 41, 56). In HaMSV genomic RNA, the presence between the 5′ cap and the v-*ras* initiation codon of MoMLV and VL30 sequences, both with stable secondary structures, indicated that the initiation of v-*ras* oncogene translation might not proceed through classical ribosome scanning (15, 41, 55). Accordingly, it has been reported that stable secondary structures present between the 5′ cap and the initiation codon can inhibit the initiation process,

most probably by preventing scanning of the 40S ribosomal subunits (27, 29, 30).

In an attempt to investigate the mechanism by which HaMSV could promote an efficient expression of the v-*ras* oncoprotein, we asked whether the 5′ VL30 sequence present in the HaMSV 5′ leader could direct efficient translation of the v-*ras* oncogene. Translation of the 5′ VL30 · *lacZ* RNAs has been performed in the RRL, and the results show that the 5′ VL30 sequence is able to confer cap-independent translation (Fig. 1). To confirm this finding, poliovirus protease 2A, which inhibits cap-dependent translation by inactivating the cap-binding complex eIF-4F (20), was coexpressed in NIH 3T3 cells with 5′ VL30 · *lacZ* RNAs. The results show that protease 2A had no effect on *lacZ* expression directed by the 5′ VL30 sequence (Fig. 3), indicating that the 5′ VL30 sequence (positions 380 to 794) allows cap-independent translation in vitro and in murine cells.

Jackson had previously reported that translation of EMCV RNA exhibited a very high KCl optimum level for an uncapped mRNA (22). This was interpreted to result from the translation initiation of this RNA via an internal ribosome entry mechanism (22). This observation prompted us to investigate the influence of KCl on the in vitro expression of 5′ VL30 · *lacZ* RNAs. The results show that the VL30 sequence from positions 380 to 794 is able to direct translation of a reporter gene in the presence of a high Cl^- concentration, which inhibits the binding of the initiating 40S ribosomal subunit to the mRNA (60) as would be required for the translation initiation by the classical ribosomal scanning mechanism.

An alternative mode of translation initiation has been described for a variety of viral and cellular mRNAs. It is a cap-independent mechanism which is promoted by an IRES, and it is well documented in naturally uncapped RNAs of picornaviruses (9, 18, 23, 24, 45, 47). The IRES element is formed of highly structured RNA domains with stretches rich in pyrimidine residues and directs ribosomes either to sequences upstream of the start codon or to the initiation codon (14, 23). This mechanism of internal initiation translation has been reported for viral RNAs, such as Friend MLV (7), hepatitis C virus (57), cowpea mosaic virus (53), turnip mosaic potyvirus (4), and murine hepatitis virus 5 (52) RNAs, and cellular RNAs such as the immunoglobulin heavy-chain binding protein mRNA (34), human fibroblast growth factor 2 mRNA (57a), and *Drosophila antennapedia* homeotic mRNA (44). To investigate the possible presence of an IRES in the HaMSV 5′ leader, dicistronic vectors were constructed and assayed in vitro and in cell culture. The results of the in vitro and in vivo experiments clearly showed that the 5′ VL30 sequence between positions 380 and 794 can efficiently direct the internal initiation of protein synthesis (Fig. 6 and 7).

Interestingly, previous studies on Friend MLV have reported that initiation of *gag* and glyco-*gag* translation (33) was controlled by an IRES located in the 5′ leader (7). The presence of an IRES in the 5′ structured leader of HaMSV and Friend MLV adjacent to or overlapping other elements critical for viral replication such as the primer binding site and the dimerization and packaging signal (E/DLS) raises interesting questions. These elements are implicated in the control of genomic RNA dimerization/packaging and v-ras^H or *gag* translation, two steps which are necessary for viral expression but appear to be mutually exclusive (8, 11). In HaMSV, deletion of the VL30 sequence containing the E/DLS resulted in an increase in IRES function in vivo (Fig. 7). In hepatitis B virus, it has been shown that the binding of the ribosomes to the encapsidation signal of the genomic RNA prevents packaging (43). Therefore, two functions of the IRES in the HaMSV 5′ leader could be to regulate the balance between v-*ras* expression and genomic RNA packaging and to permit efficient v-*ras* translation in spite of stable secondary structures and the E/DLS signal (15, 41, 53) necessary for RNA packaging into virions.

Studies on human (38) and rat (21) LINE1 retroelements suggested that an internal ribosomal entry mechanism could direct the translation initiation of the LINE1 open reading frame 2 coding for reverse transcriptase. These observations suggest that the presence of IRES in retrotransposable elements might have strong implications in the activation of proto-oncogenes. Indeed, insertion of a VL30 sequence 5′ to the c-*ras* gene could promote not only the transduction of the *ras* proto-oncogene but also a translational activation of *ras* via the IRES function (32, 35).

Identification of an IRES in the rat retrotransposon VL30 RNA led us to develop a new dicistronic MLV VL30 vector for gene transfer in which the VL30 sequence was inserted between two genes. In this retroviral vector, the VL30 IRES promotes both the efficient expression of the second gene and packaging (Fig. 8). The IRESs of EMCV and poliovirus have been used in dicistronic vectors to permit the translation of a downstream cistron (2, 17, 40). However, in these vectors, a second signal at the 5′ end was required for encapsidation of recombinant RNAs. Thus, the presence of an IRES and a retroviral packaging signal in the same element represents a major advantage of the VL30 vectors presented here. The ability to relocate the E/DLS-VL30 signal in the center of the vector favors the notion that the encapsidation function is relatively independent of neighboring sequences. However, a fourfold higher titer was produced when the E/DLS-VL30 signal was near the 5′ end of the retroviral vector, perhaps as a consequence of partial occlusion by the surrounding sequences or as an indication that the E/DLS-VL30 acts more efficiently when it can interact with the correct neighboring 5′ sequences (42). This is presently under investigation in order to further improve these MLV VL30 vectors for human gene transfer.

ACKNOWLEDGMENTS

Thanks are due to N. Fouillot for the gift of pMLP-P2A and pMLP-RP2A, to F. Flamand for the gift of pAPE, and to P. Savatier for the gift of pβ-actin-LacZ. We thank M. Lapadat-Tapolsky for a critical reading of the manuscript.

This work was supported by a grant from the Fondation Merieux, by the French association against AIDS (ANRS), the French association against cancer (ARC), and the MGEN.

REFERENCES

1. **Adam, M. A., and A. D. Miller.** 1988. Identification of a signal in a murine retrovirus that is sufficient for packaging of nonretroviral RNA into virions. J. Virol. **62:**3802–3806.
2. **Adam, M. A., N. Ramesh, A. D. Miller, and W. R. Osborne.** 1990. Internal initiation of translation in retroviral vectors carrying picornavirus 5′ nontranslated regions. J. Virol. **65:**4985–4990.
3. **Anderson, G. R., and K. C. Robbins.** 1976. Rat sequences of the Kirsten and Harvey murine sarcoma virus genomes: nature, origin, and expression in rat tumor RNA. J. Virol. **17:**335–351.
4. **Basso, J., P. Dallaire, P. J. Charest, Y. Devantier, and J.-F. Laliberté.** 1994. Evidence for an internal ribosome entry site within the 5′ non-translated region of turnip mosaic potyvirus RNA. J. Gen. Virol. **75:**3157–3165.
5. **Baudin, F., R. Marquet, C. Isel, J.-L. Darlix, B. Ehresmann, and C. Ehresmann.** 1993. Functional sites in the region of human immunodeficiency virus type 1 RNA form defined structural domains. J. Mol. Biol. **229:**382–397.
6. **Bender, M. A., T. D. Palmer, R. E. Gelinas, and A. D. Miller.** 1987. Evidence that the packaging signal of Moloney murine leukemia virus extends into the *gag* region. J. Virol. **61:**1639–1646.
7. **Berlioz, C., and J.-L. Darlix.** 1995. An internal ribosomal entry mechanism promotes translation of murine leukemia virus *gag* polyprotein precursors. J. Virol. **69:**2214–2222.

8. **Bieth, E., C. Gabus, and J.-L. Darlix.** 1990. A study of the dimer formation of Rous sarcoma virus RNA and of its effect on viral protein synthesis in vitro. Nucleic Acids Res. **18:**119–127.
9. **Borman, A., and R. J. Jackson.** 1992. Initiation of translation of human rhinovirus RNA: mapping the internal ribosome entry site. Virology **188:** 685–696.
10. **Chen, C., and H. Okayama.** 1987. High-efficiency transformation of mammalian cells by plasmid DNA. Mol. Cell. Biol. **7:**2745–2752.
11. **Coffin, J.** 1985. Structure of the retroviral genome, p. 261–368. *In* R. Weiss, N. Teich, H. Varmus, and J. Coffin (ed.), RNA tumor viruses, 2nd ed. Cold Spring Harbor Laboratory Press, Cold Spring Harbor, N.Y.
12. **Darlix, J.-L., M. Zuker, and P.-F. Spahr.** 1982. Structure-function relationship of Rous sarcoma virus leader RNA. Nucleic Acids Res. **17:**5183–5196.
13. **Dolph, P. J., J. Huang, and R. J. Schneider.** 1990. Translation by the adenovirus tripartite leader: elements which determine independence from cap-binding protein complex. J. Virol. **64:**2669–2677.
14. **Duke, G. M., M. A. Hoffman, and A. C. Palmenberg.** 1992. Sequence and structural elements that contribute to efficient encephalomyocarditis virus RNA translation. J. Virol. **66:**1602–1609.

14a. **Ehresmann, C.** Personal communication.

15. **Firulli, B. A., G. R. Anderson, D. L. Stoler, and D. E. Scott.** 1993. Anoxia-inducible rat VL30 elements and their relationship to *ras*-containing sarcoma viruses. J. Virol. **67:**6857–6862.
16. **Fouillot, N., S. Tlouzeau, J. M. Rossignol, and O. Jean-Jean.** 1993. Translation of the hepatitis B virus P gene by the ribosomal scanning as an alternative to internal initiation. J. Virol. **67:**4886–4895.
17. **Ghattas, I. R., J. R. Sanes, and J. E. Majors.** 1991. The encephalomyocarditis virus internal ribosome entry site allows efficient coexpression of two genes from a recombinant provirus in cultured cells and in embryos. Mol. Cell. Biol. **11:**5848–5859.
18. **Glass, M. J., X.-Y. Jia, and D. F. Summers.** 1993. Identification of the hepatitis A virus internal ribosome entry site: in vivo and in vitro analysis of bicistronic RNAs containing the HAV 5′ noncoding region. Virology **193:** 842–852.
19. **Harvey, J. J.** 1964. An unidentified virus which causes the rapid production of tumors in mice. Nature (London) **204:**1104–1105.
20. **Hellen, C. U. T., M. Fäcke, H.-G. Kräusslich, C.-K. Lee, and E. Wimmer.** 1991. Characterization of poliovirus 2A proteinase by mutational analysis: residues required for autocatalytic activity are essential for induction of cleavage of eukaryotic initiation factor 4F polypeptide p220. J. Virol. **65:** 4226–4231.
21. **Ilves, H., O. Kahre, and M. Speek.** 1992. Translation of the rat LINE bicistronic RNAs in vitro involves ribosomal reinitiation instead of frame-shifting. Mol. Cell. Biol. **12:**4242–4248.
22. **Jackson, R. J.** 1991. Potassium salts influence the fidelity of mRNA translation initiation in rabbit reticulocyte lysates: unique features of encephalomyocarditis virus RNA translation. Biochim. Biophys. Acta **1088:**345–358.
23. **Jackson, R. J., M. T. Howell, and A. Kaminski.** 1990. The novel mechanism of initiation of picornavirus RNA translation. Trends Biochem. Sci. **15:**477–483.
24. **Jang, S. K., H. Kräusslich, M. J. Nicklin, G. M. Duke, A. C. Palmenberg, and E. Wimmer.** 1988. A segment of the 5′ nontranslated region of encephalomyocarditis virus RNA directs internal entry of ribosomes during in vitro translation. J. Virol. **62:**2636–2643.
25. **Kalnins, A., K. Otto, U. Rütter, and B. Müller-Hill.** 1983. Sequence of the lacZ gene of Escherichia coli. EMBO J. **2:**593–597.
26. **Khandjian, E., and C. Meric.** 1986. A procedure for Northern blot analysis of native RNA. Anal. Biochem. **159:**80–85.
27. **Kozak, M.** 1986. Influences of mRNA secondary structure on initiation by eukaryotic ribosomes. Proc. Natl. Acad. Sci. USA **83:**2850–2854.
28. **Kozak, M.** 1986. Point mutations define a sequence flanking the AUG initiator codon that modulates translation by eukaryotic ribosomes. Cell **44:**283–292.
29. **Kozak, M.** 1987. Effects of intercistronic length on the efficiency of reinitiation by eukaryotic ribosomes. Mol. Cell. Biol. **7:**3438–3445.
30. **Kozak, M.** 1989. Circumstances and mechanisms of inhibition of translation by secondary structure in eucaryotic mRNAs. Mol. Cell. Biol. **9:**5134–5142.
31. **Kozak, M.** 1989. The scanning model for translation: an update. J. Cell Biol. **108:**229–241.
32. **Lang, M., I. Treinies, P. H. Duesberg, R. Kurth, and K. Cichutek.** 1994. Development of transforming function during transduction of proto-ras into Harvey sarcoma virus. Proc. Natl. Acad. Sci. USA **91:**654–658.
33. **Ledbetter, J., and R. C. Nowinski.** 1977. Identification of the gross cell surface antigen associated with murine leukemia virus-infected cells. J. Virol. **23:**315–322.
34. **Macejak, D., and P. Sarnow.** 1991. Internal initiation of translation mediated by the 5′ leader of a cellular mRNA. Nature (London) **353:**90–94.
35. **Makris, A., C. Patriotis, S. E. Bear, and P. N. Tsichlis.** 1993. Structure of a Moloney murine leukemia virus–virus-like 30 recombinant: implications for transduction of the c-Ha-*ras* proto-oncogene. J. Virol. **67:**1286–1291.
36. **Manly, K. F., G. R. Anderson, and D. L. Stoler.** 1988. Harvey sarcoma virus genome contains no extensive sequences unrelated to those of other retroviruses except *ras*. J. Virol. **62:**3540–3543.
37. **Markowitz, D., S. P. Goff, and A. Bank.** 1988. A safe packaging line for gene transfer: separating viral genes on two different plasmids. J. Virol. **62:**1120–1124.
38. **McMillan, P. P., and M. F. Singer.** 1993. Translation of the human LINE-1 element, L1Hs. Proc. Natl. Acad. Sci. USA **90:**11533–11537.
39. **Merrick, W.** 1992. Mechanism and regulation of eukaryotic protein synthesis. Microbiol. Rev. **56:**291–315.
40. **Morgan, R. A., L. Couture, O. Elroy-Stein, J. Ragheb, B. Moss, and W. F. Anderson.** 1992. Retroviral vectors containing putative internal ribosome entry sites: development of a polycistronic gene transfer system and applications to human gene therapy. Nucleic Acids Res. **20:**1293–1299.
41. **Mougel, M., N. Tounekti, J.-L. Darlix, J. Paoletti, B. Ehresmann, and C. Ehresmann.** 1993. Conformational analysis of the 5′ leader and the gag initiation site of Mo-MuLV RNA and allosteric transitions induced by dimerization. Nucleic Acids Res. **21:**4677–4684.
42. **Murphy, J. E., and S. P. Goff.** 1989. Construction and analysis of deletion mutations in the U5 region of Moloney murine leukemia virus: effects on RNA packaging and reverse transcriptase. J. Virol. **63:**319–327.
43. **Nassal, M., M. Junker-Niepmann, and H. Schaller.** 1990. Translational inactivation of RNA function: discrimination against a subset of genomic transcripts during HBV nucleocapsid assembly. Cell **63:**1357–1363.
44. **Oh, S.-K., P. S. Matthew, and P. Sarnow.** 1992. Homeotic gene Antennapedia mRNA contains 5′-noncoding sequences that confer translational initiation by internal ribosome binding. Genes Dev. **6:**1643–1653.
45. **Pelletier, J., G. Kaplan, V. R. Racaniello, and N. Sonnenberg.** 1988. Cap-independent translation of poliovirus mRNA is conferred by sequence elements within the 5′ noncoding region. Mol. Cell. Biol. **8:**1103–1112.
46. **Pelletier, J., G. Kaplan, V. R. Racaniello, and N. Sonnenberg.** 1988. Translational efficiency of poliovirus mRNA: mapping inhibitory *cis*-acting elements within the 5′ noncoding region. J. Virol. **62:**2219–2227.
47. **Pelletier, J., and N. Sonnenberg.** 1988. Internal initiation of translation of eukaryotic mRNA directed by a sequence derived from poliovirus RNA. Nature (London) **334:**320–325.
48. **Rotman, G., A. Itin, and E. Keshet.** 1986. Promoter and enhancer activities of long terminal repeats associated with cellular retrovirus-like (VL30) elements. Nucleic Acids Res. **14:**645–658.
49. **Sambrook, J., E. F. Fritsch, and T. Maniatis.** 1989. Molecular cloning: a laboratory manual, 2nd ed. Cold Spring Harbor Laboratory Press, Cold Spring Harbor, N.Y.
50. **Savatier, P., J. Morgenstern, and R. S. P. Beddington.** 1990. Permissiveness to murine leukemia virus expression during preimplantation and early postimplantation mouse development. Development **109:**655–665.
51. **Swain, A., and J. M. Coffin.** 1992. Mechanism of transduction by retroviruses. Science **255:**841–845.
52. **Thiel, V., and S. G. Siddell.** 1994. Internal ribosome entry in the coding region of murine hepatitis virus mRNA 5. J. Gen. Virol. **75:**3041–3046.
53. **Thomas, A. M., E. ter Haar, K. Wellink, and H. O. Voorma.** 1991. Cowpea mosaic virus middle component RNA contains a sequence that allows internal binding of ribosomes and that requires eukaryotic initiation factor 4F for optimal translation. J. Virol. **65:**2953–2959.

53a. **Torrent, C.** Unpublished data.

54. **Torrent, C., T. Bordet, and J.-L. Darlix.** 1994. Analytical study of rat retrotransposon VL30 RNA dimerization in vitro and packaging in murine leukemia virus. J. Mol. Biol. **240:**434–444.
55. **Torrent, C., C. Gabus, and J.-L. Darlix.** 1994. A small and efficient dimerization/packaging signal of rat VL30 RNA and its use in murine leukemia virus-VL30-derived vectors for gene transfer. J. Virol. **68:**661–667.
56. **Tounekti, N., M. Mougel, C. Roy, R. Marquet, J.-L. Darlix, J. Paoletti, B. Ehresmann, and C. Ehresmann.** 1992. Effect of dimerization on the conformation of the encapsidation Psi domain of Moloney murine leukemia virus RNA. J. Mol. Biol. **223:**205–220.
57. **Tsukiyama-Kohara, K., N. Iizuka, M. Kohara, and A. Nomota.** 1992. Internal ribosome entry site within hepatitis C virus RNA. J. Virol. **66:**1476–1483.

57a. **Vagner, S., M.-C. Gensac, A. Maret, F. Bayard, F. Amalric, H. Prats, and A.-C. Prats.** 1995. Alternative translation of human fibroblast growth factor 2 mRNA occurs by internal entry of ribosomes. Mol. Cell. Biol. **15:**35–44.

58. **Velu, T. J., W. C. Vass, D. C. Lowy, and P. E. Tambourin.** 1989. Harvey murine sarcoma virus: influences of coding and noncoding sequences on cell transformation in vitro and oncogenicity in vivo. J. Virol. **63:**1384–1392.
59. **Weber, L. A., E. D. Hickey, and C. Baglioni.** 1978. Influence of potassium salt concentration and temperature on inhibition of mRNA translation by 7-methylguanosine 5′-monophosphate. J. Biol. Chem. **253:**178–183.
60. **Weber, L. A., E. D. Hickey, P. A. Maroney, and C. Baglioni.** 1977. Inhibition of protein synthesis by Cl^-. J. Biol. Chem. **252:**4007–4010.
61. **Wei, C. M., D. R. Lowy, and E. M. Scolnick.** 1980. Mapping of transforming region of the Harvey murine sarcoma virus genome by using insertion-deletion mutants constructed in vitro. Proc. Natl. Acad. Sci. USA **77:**4674–4678.
62. **Weiss, R., N. Teich, H. Varmus, and J. Coffin.** 1985. RNA tumor viruses, 2nd ed., p. 928–931. Cold Spring Harbor Laboratory Press, Cold Spring Harbor, N.Y.